Contents lists available at ScienceDirect

Science of the Total Environment

journal homepage: http://ees.elsevier.com

Climate change impact assessment on the hydrology of a large river basin in Ethiopia using a local-scale climate modelling approach

Solomon H. Gebrechorkos [a,b,*], Christian Bernhofer [c], Stephan Hülsmann [a,d]

[a] School of Geography and Environmental Science, University of Southampton, United Kingdom
[b] United Nations University Institute for Integrated Management of Material Fluxes and of Resources (UNU-FLORES), Dresden, Germany
[c] Faculty of Environmental Sciences, Institute of Hydrology and Meteorology, Technische Universität Dresden, Germany
[d] Global Change Research Institute CAS, 603 00 Brno, Czech Republic

ARTICLE INFO

Article history:
Received 29 April 2020
Received in revised form 22 June 2020
Accepted 23 June 2020
Available online xxx
Editor: Ashantha Goonetilleke

Keywords
Climate projection
SDSM
Climate change
Hydro-climate modelling
Impact assessment
Awash Basin

ABSTRACT

Local-scale climate change adaptation is receiving more attention to reduce the adverse effects of climate change. The process of developing adaptation measures at local-scale (e.g., river basins) requires high-quality climate information with higher resolution. Climate projections are available at a coarser spatial resolution from Global Climate Models (GCMs) and require spatial downscaling and bias correction to drive hydrological models. We used the hybrid multiple linear regression and stochastic weather generator model (Statistical Down-Scaling Model, SDSM) to develop a location-based climate projection, equivalent to future station data, from GCMs. Meteorological data from 24 ground stations and the most accurate satellite and reanalysis products identified for the region, such as Climate Hazards Group InfraRed Precipitation with Station Data were used. The Soil Water Assessment Tool (SWAT) was used to assess the impacts of the projected climate on hydrology. Both SDSM and SWAT were calibrated and validated using the observed climate and streamflow data, respectively. Climate projection based on SDSM, in one of the large and agricultural intensive basins in Ethiopia (i.e., Awash), show high variability in precipitation but an increase in maximum (Tmax) and minimum (Tmin) temperature, which agrees with global warming. On average, the projection shows an increase in annual precipitation (>10%), Tmax (>0.4 °C), Tmin (>0.2 °C) and streamflow (>34%) in the 2020s (2011–2040), 2050s (2041–2070), and 2080s (2071–2100) under RCP2.6-RCP8.5. Although no significant trend in precipitation is found, streamflow during March–May and June–September is projected to increase throughout the 21 century by an average of more than 1.1% and 24%, respectively. However, streamflow is projected to decrease during January–February and October–November by more than 6%. Overall, considering the projected warming and changes in seasonal flow, local-scale adaptation measures to limit the impact on agriculture, water and energy sectors are required.

1. Introduction

Local-scale climate change adaptation is receiving more attention to reduce the adverse effects of climate change on sectors such as agriculture and water resources. Globally, climate change is becoming one of the major challenges for achieving food, energy and water security and the impact is high in developing countries due to their limited adaptive capacity and poor management of environmental resources (Adhikari et al., 2015; Niang et al., 2014). As a result of variability and change in climate, extreme events are becoming more frequent with a significant impact on different sectors such as agriculture, energy and food systems (Brown and Funk, 2008; IPCC, 2013). Under global warming, the hydrological cycle is expected to intensify which will result in frequent floods and droughts affecting the ecosystem services and water resources (Haile et al., 2020; Wu et al., 2013). According to Wang et al. (2019), the direct impact of climate change on the hydrological cycle is due to an increase in temperature and high variability, particularly inter-annual variability, and shift in rainfall at different scales.

During the last few decades, globally and in Africa temperature has increased by about 0.72 °C (IPCC, 2013) and more than 0.5 °C, respectively and it was significant during the last three decades (Adhikari et al., 2015). In East Africa, maximum and minimum temperature observed after 1990 and 2000, respectively are warmer than the mean of the period from 1979 to 2012. Temperature extremes, which cause a significant impact on the environment, showed an increase in warm

* Corresponding author at: School of Geography and Environmental Science, University of Southampton, United Kingdom.
E-mail address: gebrechorkos@unu.edu (S.H. Gebrechorkos)

https://doi.org/10.1016/j.scitotenv.2020.140504
0048-9697/

(e.g., warm days and summer days) and decrease in cold (cold nights and cold spell duration) indices (Camberlin, 2017; Cattani et al., 2018; Gebrechorkos et al., 2018a). Climate projections in East Africa and globally also show an increase in temperature and high variability in rainfall, which might cause a significant impact on the hydrological cycle and lead to extreme events (e.g, heavy rainstorms, floods, hurricanes and droughts) will be more frequent (Gebrechorkos et al., 2019b; Girvetz et al., 2019; IPCC, 2013). Hence, considering the current and future changes in climate development of adaptation measures is urgently needed to minimize the impact on agriculture, on which more than 80% of the people in East Africa depend (FAO, 2014), but also on water resources and energy sectors.

Hydrological impacts of climate change on a basin and watershed-scale are typically assessed using climate projections based on different climate change scenarios (e.g., Guo et al., 2020; Luo et al., 2013; Schnorbus and Cannon, 2014). The typical approach is to use climate change projections from Global Climate Models (GCMs) driven by defined emission scenarios identifying paths of radiative forcings or greenhouse gas emissions. Climate projections from GCMs provide the best possible information to assess changes and variability in climate on a global scale (IPCC, 2007, 2013). However, the output from GCMs is spatially too coarse (>100 km) to be used in hydrological models to assess climate change impacts at a local and regional scale (e.g., watershed) and it is associated with large uncertainties (Luo et al., 2013). Therefore, climate projections from GCMs require spatial downscaling before application in sector models such as hydrological modelling (Gutmann et al., 2012; Tavakol-Davani et al., 2012). Application of GCMs, in addition to the coarse resolution, in impact assessment studies is limited due to large biases, errors, and uncertainties in representing future and current climate, particularly the accuracy is low at a local and regional scales (Gebrechorkos et al., 2019b; Joetzjer et al., 2013; Lutz et al., 2016). However, impact assessment models (e.g., hydrological models) require high-resolution climate data products, equivalent to future station data, downscaled from GCMs based on field-based ground observations (Wilby and Dawson, 2013). To develop a high-resolution climate projection from GCMs, downscaling methods have been introduced (Coulibaly et al., 2005; Wilby and Dawson, 2004).

Downscaling techniques classified as dynamical (regional climate modelling) and statistical methods are used to bridge the resolution gaps between GCMs and impact models by transferring change in large-scale climate variables (e.g., mean sea level pressure) to local-scale variables (e.g., precipitation). According to Fowler and Wilby (2007), statistical downscaling methods identify a potential source of bias in climate models and improve the reliability of simulated changes in climate. Statistical methods, compared to dynamical models, are more appropriate when station data for impact assessment or extreme events are required and resources are limited (Goodess et al., 2012). In East Africa, the accuracy of dynamically downscaled data (compared to station data) is very low (e.g., low correlation and high errors and biases) while statistically downscaled data showed lower biases when compared to dynamical models and GCMs (Gebrechorkos et al., 2018b, 2019b; Mejia et al., 2012). Mejia et al. (2012) concluded that GCMs cannot be expected to accurately represent future climate changes at a local scale as they are designed for assessing climate variability and climate changes impacts on a global scale.

Statistical downscaling models, on the other hand, produce daily weather series which are more appropriate for impact assessment models such as hydrological models (Brown and Funk, 2008; Khan and Coulibaly, 2009). The application of statistically downscaled climate projections in hydrological models is considered as the most reliable method to assess the impact of climate change in hydrology and for projecting a future change in climate on a regional and local scale (Schnorbus and Cannon, 2014). Considering the reliability and suitability of the statistical downscaling models in hydrological modelling, in this study, the Statistical DownScaling Model (SDSM) (Wilby and Dawson, 2004) was used to downscale projections from a GCM and three Representative Concentration Pathways (RCPs; RCP2.6, RCP4.5, and RCP8.5). SDSM is a hybrid of a stochastic weather generator and transfer functions (Wilby and Dawson, 2004) because large scale variables (circulation patterns and atmospheric moisture) are used to condition predictands (local climate variables) and artificially inflate the variance and improve the downscaled data (Wilby and Dawson, 2013). SDSM is one of the most widely used downscaling models for precipitation and temperature and its performance is higher than other weather generators (Hashmi et al., 2011; Hassan et al., 2013). Moreover, SDSM possesses higher skills in generating daily rainfall characteristics (e.g., wet and dry days), maximum and minimum temperature and inter-annual climate variability compared to other statistical downscaling methods such as weather generators (Wilby and Dawson, 2004; Hassan et al., 2013; Liu et al., 2015; Tryhorn and DeGaetano, 2011; Liu et al., 2011; Behera et al., 2016). We focused on the Awash River basin as one of the most agricultural intensive and economically important basins in Ethiopia. Due to the limited availability of ground observation from field-based meteorological stations, we used additional climate data products (i.e., based remote sensing and reanalysis data) recommended for the region after a comprehensive data evaluation in East Africa (Gebrechorkos et al., 2018b) and sub-basins of Ethiopia and Kenya (Ayugi et al., 2019; Basheer and Elagib, 2019).

In order to assess the added values of the additional climate data products in hydrological modelling, the hydrological model Soil Water Assessment Tool (SWAT) was used. The model is calibrated and validated with and without the additional datasets. In addition to providing a detailed analysis of the hydrological changes, the result will help effective management and planning of water resources and to accurately assess the timing and volume of future streamflow in the basin, which has hitherto not been assessed in a detailed manner. Limited studies inside and around the basin (Berhe et al., 2013; Tadese et al., 2019) argued that the current and future climate change might worsen the water availability for irrigation with an increasing frequency of dry spells. Hence, it is recommended to develop adaptation and management strategies and methods to improve water allocation systems, particularly during dry seasons. The result will help in designing hydrological structures such as dams and river diversions and develop sustainable and site-specific adaptation measures to reduce the impact of climate change on agriculture, energy and other sectors.

2. Material and methods

2.1. Study area

The study was conducted in the Awash basin located in the northeastern part of Ethiopia between longitudes 37.8°E and 41.3°E and latitudes 7.89°N and 11.87°N (Fig. 1). The Awash basin is one of the 12 largest river basins in Ethiopia with a total area of about 110,000 km^2 of which 61,032.58 km^2 are considered in this study due to the limited availability of climate and hydrological data for model calibration and validation. According to Ayenew et al. (2008), the origin of the basin is from the Shewa highlands with an altitude of about 3000 m.a.s.l. Awash is one of the most economically important river basins in Ethiopia with an irrigation area of about 70% of the region's agricultural land (Hirpa et al., 2009). This is one of the most utilized and early developed basins in terms of applications of modern agriculture systems (Berhe et al., 2013). The basin hosts more than 18 million people, mostly smallholder farmers (Taye et al., 2018), dependent on the agriculture sector which makes water management, particularly during the dry season, very important. The drier and wetter (main rainy seasons) months are January–February (JF) and October–Decem-

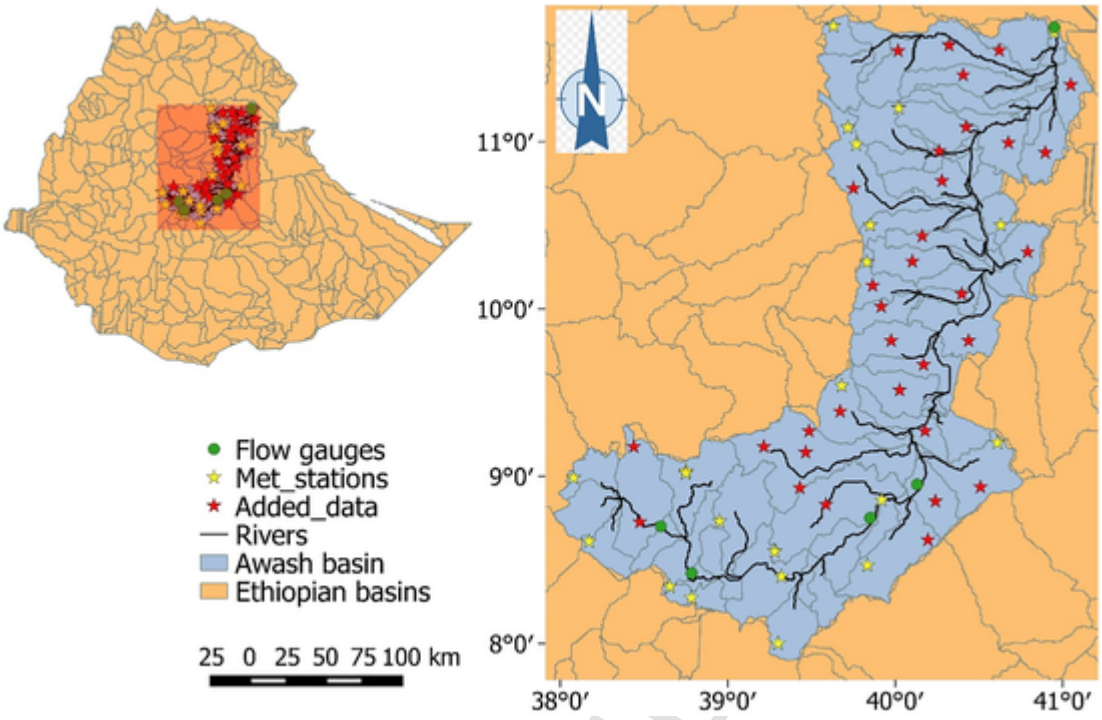

Fig. 1. Location map of the Awash river basin and ground stations; the polygons are hydrological basins.

ber (OND) and March–May (MAM) and June–September (JJAS), respectively. OND and MAM are also known as the short and long rainy season (Taye et al., 2018).

Due to the diverse topography, with elevation ranging from 3600 m.a.s.l in the western part to 250 m.a.s.l in the eastern part, the climate, particularly seasonal rainfall, is highly variable. In addition, seasonal rainfall distribution in the basin is highly influenced by the movement of large scale climate variables such as the Inter-Tropical Convergence Zone (ITCZ). The area is characterized mainly by two wet seasons starting from March to May (spring) and July–September (summer) (Berhe et al., 2013). The average annual temperatures of the basin range from 16.7 °C in the upper part of the basin around Addis Ababa to 29 °C in the eastern part around Djibouti. Moreover, the average annual rainfall ranges from 200 to 1600 mm in the eastern parts around Afar depression and the highlands in the western part of the basin, respectively (Ayenew et al., 2008).

2.2. Datasets

In this study, multiple datasets, climate and hydrological data, from different sources were used. Observed daily rainfall and maximum and minimum temperature (Tmax and Tmin) from 24 field-based meteorological stations obtained from the National Meteorological Agency of Ethiopia and daily and monthly streamflow data from Ethiopian Ministry of Agriculture were used. Compared to the basin size and complex topography, the number of stations is very limited to develop a representative hydrological model and we used 31 additional data, equivalent to station data, extracted from satellite- and reanalysis based climate data products (precipitation, Tmax, and Tmin). For East Africa, we have evaluated multiple climate data products on daily-monthly time scales for application in hydro-climate studies in areas where ground station data is limited (Gebrechorkos et al., 2018b). From the evaluation, two datasets, the Climate Hazards Group InfraRed Precipitation with Station data (CHIRPS (Funk et al., 2015)) and Observational-Reanalysis Hybrid (ORH (Sheffield et al., 2006)), were found the most accurate datasets for precipitation and Tmax and Tmin, respectively. Moreover, wind, solar radiation, and relative humidity were used from the National Centers for Environmental Prediction Climate Forecast System Reanalysis (NCEP-CFSR, https://rda.ucar.edu/pub/cfsr.html).

CHIRPS is a quasi-global satellite-based precipitation product developed for managing and monitoring of extreme events (e.g., droughts) and trend analysis (Funk et al., 2015). The product is available at a high spatial resolution (0.05°) and multiple time scales (daily-monthly) from 1981-present. CHIRPS is freely available at the Climate Hazards Center University of California, Santa Barbara (CHG; ftp://ftp.chg.ucsb.edu/pub/org/chg/products/CHIRPS-2.0). The product is developed from a 0.05° satellite imagery, Climate Hazards Center's Precipitation Climatology version 1 (CHPclim), and ground station data. In East Africa, CHIRPS is used as input in hydrological modelling and climate projection to assess current and future hydro-climate changes and climate change trend analysis (Fenta et al., 2017; Funk et al., 2015; Gebrechorkos et al., 2019b).

ORH also called Princeton Global Forcings (PGF), is a widely used global climate dataset developed by spatial and temporal downscaling of the most widely used reanalysis, National Centers for Environmental Prediction–National Center for Atmospheric Research (NCEP–NCAR), data into different spatial (up to 0.1°) and temporal resolution (up to 3-hourly). Multiple products are included in the development of ORH such as Tropical Rainfall Measuring Mission (TRMM), Global Precipitation Climatology Project (GPCP) and ground observations. The data is corrected for biases and random errors and temporal in-homogeneities are removed using gap-filled and quality controlled ground stations data (Chaney et al., 2014; Sheffield et al., 2006). The data is available at multiple time scales and spatial resolution from the Terrestrial Hydrology Research Group, Princeton University (http://hydrology.princeton.edu/data.pgf.php). In addition to the climate data, observed daily streamflow data from five stations, for model calibration and validation, were obtained from the Global Runoff Database (GRDC)–Bfg (Global Runoff Data Centre, 2019) for the period 1990–2009. GRDC is an international hydrological data archive (https://www.bafg.de/

GRDC/EN/01_GRDC/) designed to support scientists assess global changes in climate and its risks and impacts on the environment.

The NCEP-CSFR is the third generation high resolution (~38 km) reanalysis dataset available from 1979 to 2014 in SWAT file format at the Global Weather Data for SWAT (https://globalweather.tamu.edu). The product is based on a coupled atmosphere-ocean-land surface-sea ice system designed to provide the best estimate of the global domain and it was found to be a very good, as good as and better than models forced by station data, product for hydrological modelling in data-sparse and different hydroclimate regions such as in Ethiopia and USA (Dile and Srinivasan, 2014; Fuka et al., 2014). Due to the availability of the data at a high spatial and temporal resolution, it provides an opportunity to develop representative hydrological modells in un-gauged basins and to advance real-time hydrological forecasting (Fuka et al., 2014). In this study, therefore, 130 data points covering the basin are extracted from the NCEP-CSFR for wind speed, solar radiation, and relative humidity, which is unavailable in the study area.

Further, we used high resolution (20-m) land use map developed by the European Space Agency (ESA, http://2016africalandcover20m.esrin.esa.int/) based on Sentinel-2A satellite observations. The land-use map shows that a large part of the basin is used for agriculture. Besides, the 30-meter Shuttle Radar Topography Mission (SRTM, http://srtm.csi.cgiar.org/srtmdata/) elevation data (DEM) from the CGIAR - Consortium for Spatial Information (CGIAR-CSI) and the 30 arc-second soil data (Fischer et al., 2008) from the Food and Agriculture Organization (FAO) Harmonised world soil database (http://www.fao.org/fileadmin/user_upload/soils/HWSD%20Viewer/HWSD.mdb) were used. The DEM shows an elevation from 394 m.a.s.l (around the outlet) to 4201 m.a.s.l in the western part of the basin. Moreover, the soil and land use maps of the basin show 17 types of soil and 9 land use classes, respectively.

2.3. Statistical downscaling of global climate projection

To develop a station based climate projection and assess the possible impacts of future climate on the hydrology, the most widely used Statistical Down-Scaling Models (SDSM) (Wilby and Dawson, 2004), was used. SDSM, also known as a hybrid of transfer function and stochastic weather generators, enables the synthesis of daily weather series in places where ground observation is available for model calibration and validation. The weather generator in SDSM allows to produce up to 100 ensembles of daily series of climate variables for the historical (e.g., 1961–2005) and future (e.g., 2006–2100) climate depending on the length of input variables. In this study, we used the mean of 20 ensembles. Downscaling in SDSM is done by developing a statistical relationship between large-scale (predictors) and local-scale (predictand) climate variables. Predictors are variables that have a predictive skill for a given predictand (Wilby and Dawson, 2004). In this study, we used all the 26 predictors developed based on the NCEP (National Centers for Environmental Prediction) reanalysis data for historical (1961–2005) and second-generation Canadian Earth System Model (CanESM2) for the historical and future (2006–2100) climate. For future climate, the predictors are available under three RCPs (RCP2.6, RCP4.5, and RCP8.5). The predictors were obtained from the Canadian Climate Data and Scenarios (http://climate-scenarios.canada.ca/?page=statistical-downscaling), which are available at a spatial resolution of about 2.81°. The predictor values approximately correspond to the centre of the GCM grid-box and the study area lies in four GCM grid boxes. The NCEP and CanESM2 predictors were used for model calibration (1961–1990) and validation (1991–2005) and future projection, respectively. A list of the predictors is provided in the supplement (ST. 1).

In SDSM the observed data is used to screen the predictors for a particular predictand (e.g., precipitation) at a give location. The predictors are selected based on the correlation and partial correlation matrix and probability value (*P*-value, which is lower than 0.05 indicating the relationship is significant). Finally, selected predictors are used to calibrate the model at monthly, seasonal and annual time-scale depending on the length of the observed data. The performance of SDSM in synthesizing the current climate was evaluated against the observed data using different statistical methods such as correlation and bias analysis. The downscaled data, for East Africa, is freely available from 1961 to 2005 (current climate) and 2006–2100 (future climate) under RCP2.6, RCP4.5, and RCP8.5 (Gebrechorkos et al. (2019c), https://doi.org/10.6084/m9.figshare.c.4282226) and it is used for climate change and impact assessment studies in basins of East Africa (Gebrechorkos et al., 2019a, 2019b).

2.4. Hydrological model setup

The Soil Water Assessment Tool (SWAT) model, particularly the ArcGIS extension of SWAT (ArcSWAT), was used to assess the current and future streamflow changes in the Awash basin. SWAT is a spatially distributed, process- and physically-based, and a continuous-time model designed to simulate quantity and quality of surface and sub-surface water on a daily time scale and predict the environmental impacts of climate change and land use and management practices (Neitsch et al., 2011). The model can be used in very large basins with different management practices in a very efficient manner (both time and cost) and its efficiency (e.g., running time) allows assessing long term impacts without spanning over several decades (Neitsch et al., 2011). In a given watershed, SWAT uses HRU's (hydrological response units) classified by a specific soil type, land cover, and slope class, which describes the spatial heterogeneity within the catchment area. According to Bosch et al. (2011), the model is effective in predicting hydrological variables and sediment yield in a range of watersheds and different characteristics. The hydrological variables simulated by SWAT include streamflow, sediment yield, evapotranspiration, groundwater recharge, and soil-water for each HRU based on the water balance equation (Eq. (1)).

$$SW_t = SW_0 + \sum_{i=1}^{t} \left(R_{day} - Q_{surf} - E_a - w_{seep} - Q_{gw}\right) \quad (1)$$

For a given time (e.g., day), SW_0 and SW_t are the initial and final soil water content (mm), R_{day} is daily precipitation (mm), Q_{surf} is surface runoff (mm), E_a is Evapotranspiration (mm), w_{seep} is seepage loss (mm) and Q_{gw} is groundwater flow (mm) (Neitsch et al., 2011).

2.5. Model calibration and evaluation

In data-sparse regions, such as countries of East Africa, developing a representative hydrological model (e.g., in generating the observed streamflow) is very challenging but it is a prerequisite to accurately assess the possible impacts of future climate. In this study, therefore, we used a combination of datasets to calibrate and validate the hydrological model. As explained in Section 2.1, in addition to the field-based ground stations, we added 31 data points, equivalent to station data, for precipitation (from CHIRPS) and Tmax and Tmin (from ORH) to improve the hydrological model accuracy during both calibration and validation. The data points were extracted based on the method described by Gebrechorkos et al. (2018b), i.e., area average instead of pixel value, which showed a higher correlation and lower bias and errors when compared to station data.

For model calibration and validation, the observed daily and monthly streamflow data were dived into two periods; 1990–2000 and 2001–2009, respectively. To assess the added values of the additional climate datasets and evaluate the model performance, the most widely

used statistical methods such as the Nash-Sutcliffe efficiency (NSE), coefficient of determination (R^2) and percent of bias (Pbias) were used. NSE (Eq. (2)) is a normalised statistics, ranges from $-\infty$ to 1, used to indicate the relative value of residual variance compared to the variance of the observed data and values close to one shows a perfect match of the modelled with the observed data (Nash and Sutcliffe, 1970). R^2 (Eq. (3)) is the square of the correlation coefficient between the observed and modelled data and values close to one shows the ability of the model to accurately predict the observed values. The Pbias (Eq. (4)), on the other hand, measures the tendency of the model values to be smaller (underestimation) or larger (overestimation) than the observed values and values close to zero indicate the most accurate model simulation.

$$NSE = 1 - \frac{\sum_{i=1}^{N}(x_i - y_i)^2}{\sum_{i=1}^{N}(x_i - \bar{x})^2} \quad (2)$$

$$R^2 = \left[\frac{\sum_{i=1}^{N}(x_i - \bar{x})\ (y_i - \bar{y})}{\sqrt{\sum_{i=1}^{N}(x_i - \bar{x})^2}\sqrt{\sum_{i=1}^{N}(y_i - \bar{y})^2}}\right]^2 \quad (3)$$

$$Pbias = \frac{\sum_{i=1}^{N}(y_i - x_i)}{\sum_{i=1}^{N}x_i} \times 100 \quad (4)$$

where x and y and $\bar{x}$ and $\bar{y}$ are modelled and observed and mean modelled and observed streamflow, respectively, N is the number of data pairs. In addition to the SWAT calibration helper, the SWAT Calibration and Uncertainty Programs (SWAT-CUP) (Abbaspour, 2015) was used during calibration, validation, and uncertainty analysis.

3. Results

3.1. Statistical downscaling using SDSM

The performance of SDSM in synthesizing the observed data from 24 ground stations and 31 data points extracted from CHIRPS and ORH was evaluated using the methods included in SDSM and described in Section 3.3. For the total 55 points, the predictors were screened 4290 times and the model was calibrated and validated 165 times (55 stations * 3 variables). For this basin, zonal wind component and specific humidity were found as the most common predictors for precipitation, T-max and T-min. In general, for a single station, we found 2–6 predictors with high correlation and statistically significant (P-value <0.05). For station Addis-Abeba, for example, the following predictors were selected: ncepp1_ugl (1000 hPa Zonal wind component), ncepp5_ugl (500 hPa Zonal wind component), nceps500gl (500 hPa Specific humidity), ncepp1thgl (1000 hPa Wind direction), ncepshumgl (1000 hPa Specific humidity), and ncepp850gl (850 hPa Geopotential). They were found to show a correlation of greater than 95% (Fig. 2) for monthly values. The model captures very well precipitation during March–May (long-rainy season) and October–December (short rainy season) but shows under and overestimation during June–September (locally called Kiremt), respectively (Fig. 2). In general, the selected predictors for all the stations show a monthly correlation of greater than 87% during the calibration (1961–1990) and validation (1991–2005) periods. Due to the complex topography of the study area, selected predictors vary from place to place. Compared to Tmax and Tmin, the correlation is lower for precipitation, particularly in stations with fewer number observations during the calibration and validation periods.

3.2. Added values of satellite and reanalysis based climate datasets in hydrological modelling

We have used satellite and reanalysis based precipitation and temperature datasets in the data-sparse part of the basin to improve the accuracy of the hydrological model and to develop a location-based climate projection. To assess the added values on the hydrological model, we compared the calibration and validation results of using only the observed data from 24 stations and with the additional 31 data points. The results show an increase in model accuracy with an increase in R^2 and NSE and decrease in Pbias in the five hydrological stations used (Table 1). For example, at station Melka-Kuntrea the model without and with the additional data showed an R^2 (NSE) of 0.67 (0.67) and 0.86 (0.84), respectively. In addition, the model bias is decreased from 13.9% to 12.5% when using more information. Moreover, the mean monthly simulated flows at Melka-Kuntrea (Hombole) improved from 21 m^3/s (27 m^3/s) to 24.6 m^3/s (47.2) while the observed flow is 26.8 m^3/s (45 m^3/s). Even though the model performance decreases,

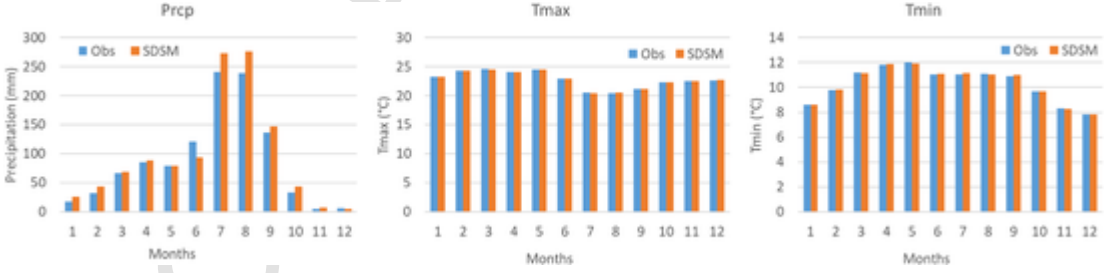

Fig. 2. Comparison of observed (Obs) and modelled (SDSM) monthly precipitation and monthly average Tmax and Tmin during 1961–2005 for station Addis-Abeba.

Table 1
Evaluation of model performance with and without using additional climate data during calibration and validation.

Stations	Area (km ^{2})	Location		Average annual flow (m ^{3}/s)	Calibration (without)			Calibration (with)			Validation (with)		
		lat	lon		R^2	NSE	Pbias	R^2	NSE	Pbias	R^2	NSE	Pbias
Melka-Kuntrea	4456	8.7	38.6	390	0.67	0.67	13.9	0.86	0.84	12.5	0.72	0.62	29.1
Hombole	4656	8.4	38.8	420	0.59	0.31	64.8	0.79	0.75	26.3	0.69	0.58	67.1
Metehara	16,416	8.8	39.9	550	0.33	0.28	75.6	0.47	0.42	13.5	0.39	0.33	9.3
Melka-Selki	21,520	9.4	40.1	610	0.21	0.19	69.8	0.49	0.4	28.5	0.38	0.31	23.2
Tendaho	62,088	11.7	41	860	0.19	0.11	79.2	0.39	0.37	55.7	0.38	0.36	66.4

due to limited hydrological information, with an increase in the drainage area, it showed an improved R^2 and NSE and decrease in Pbias with additional climate data both during calibration and validation. At station Tendaho (outlet) both NSE and R^2 increased from 0.19 and 0.11 to 0.39 and 0.35, respectively and Pbias decreased from 79.2 to 55.7. During validation, similar to calibration, the models showed high R^2 and NSE values and lower bias in all the hydrological stations with the additional data. Overall, the results show an improved model performance when additional climate data with high spatial and temporal resolution and accuracy are used.

3.3. Projected changes in climate and streamflow

To assess the possible changes in climate (precipitation, Tmax, and Tmin), the period 1961–1990 was used as baseline (reference) period and anomalies were computed, as a departure from the mean, for each variable. For analysis, the projection period is divided into the 2020s (2011–2040), 2050s (2041–2070), and 2080s (2071–2100). The results show an increase in Tmax and Tmin and precipitation in large parts of the basin (Figs. 3–6). In the 2020s, the basin Tmax will be warmer (up to 1.45 °C, particularly in the southwest) and colder (up to −0.3 °C) than during the baseline period under the RCPs with a higher change under RCP8.5 compared to RCP2.6 and RCP4.5 (Fig. 3). Similar to the 2020s, Tmax will be warmer (up to 2.7 °C) compared to the baseline period in the southwestern part of the basin in the 2050s and will continue to increase (up to 3.7 °C) in the 2080s. Taking the basin average (Fig. 6), Tmax will be higher than during the baseline period in the 2020s, 2050s, and 2080s. In the 2020s, Tmax is projected to increase by an average of 0.44 °C, 0.46 °C, and 0.47 °C under RCP2.6, RCP4.5, and RCP8.5, respectively. In addition, the change in Tmax will be higher in the 2050s (2080s) by 0.57 °C (0.54 °C), 0.67 °C (0.76 °C), and 0.88 °C (1.30 °C) compared to the baseline period.

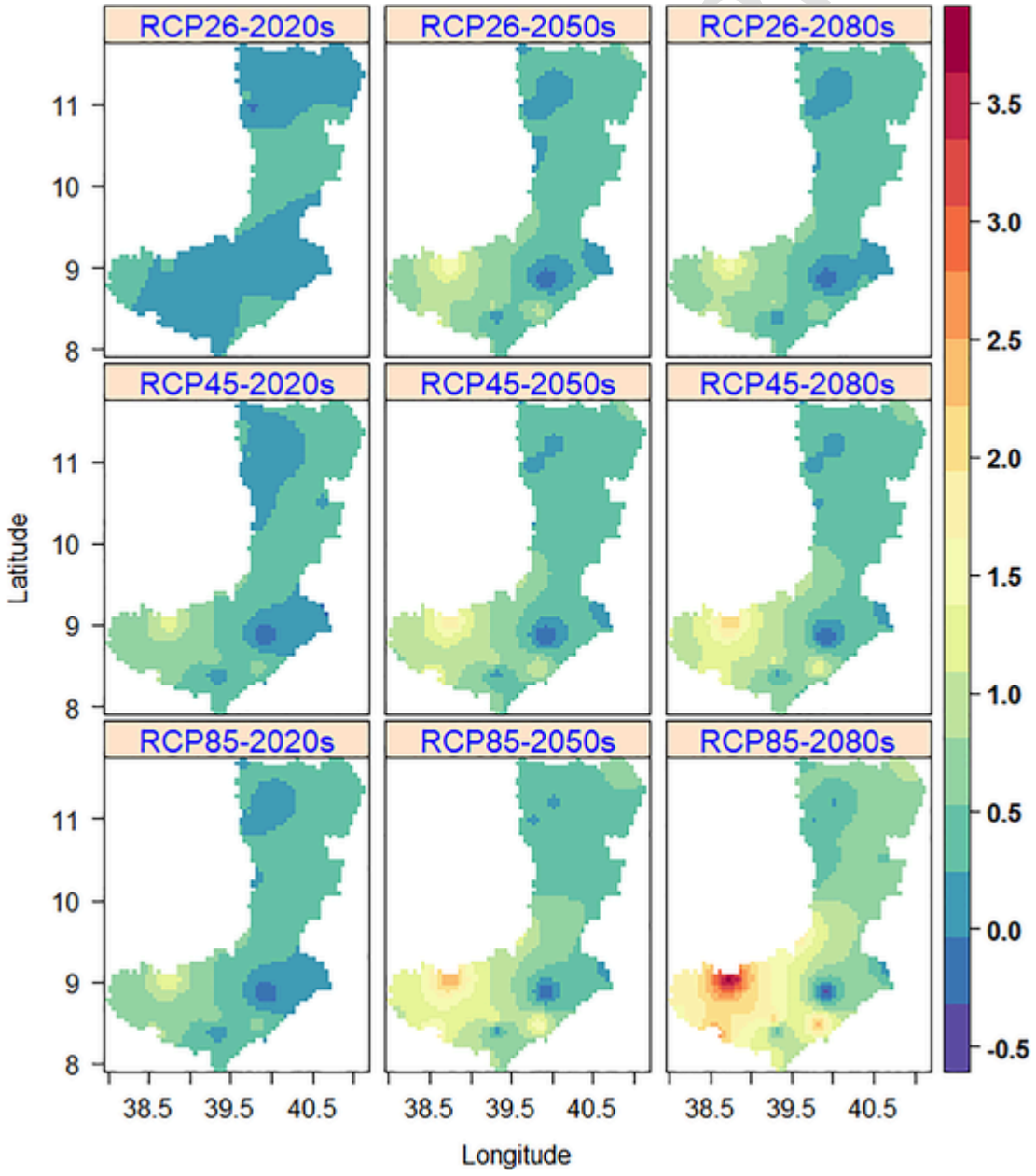

Fig. 3. Projected changes in Tmax (°C) in 2020s (right), 2050s (middle), and 2080s (left) under RCP2.6 (upper), RCP4.5 (middle), and RCP8.5 (lower).

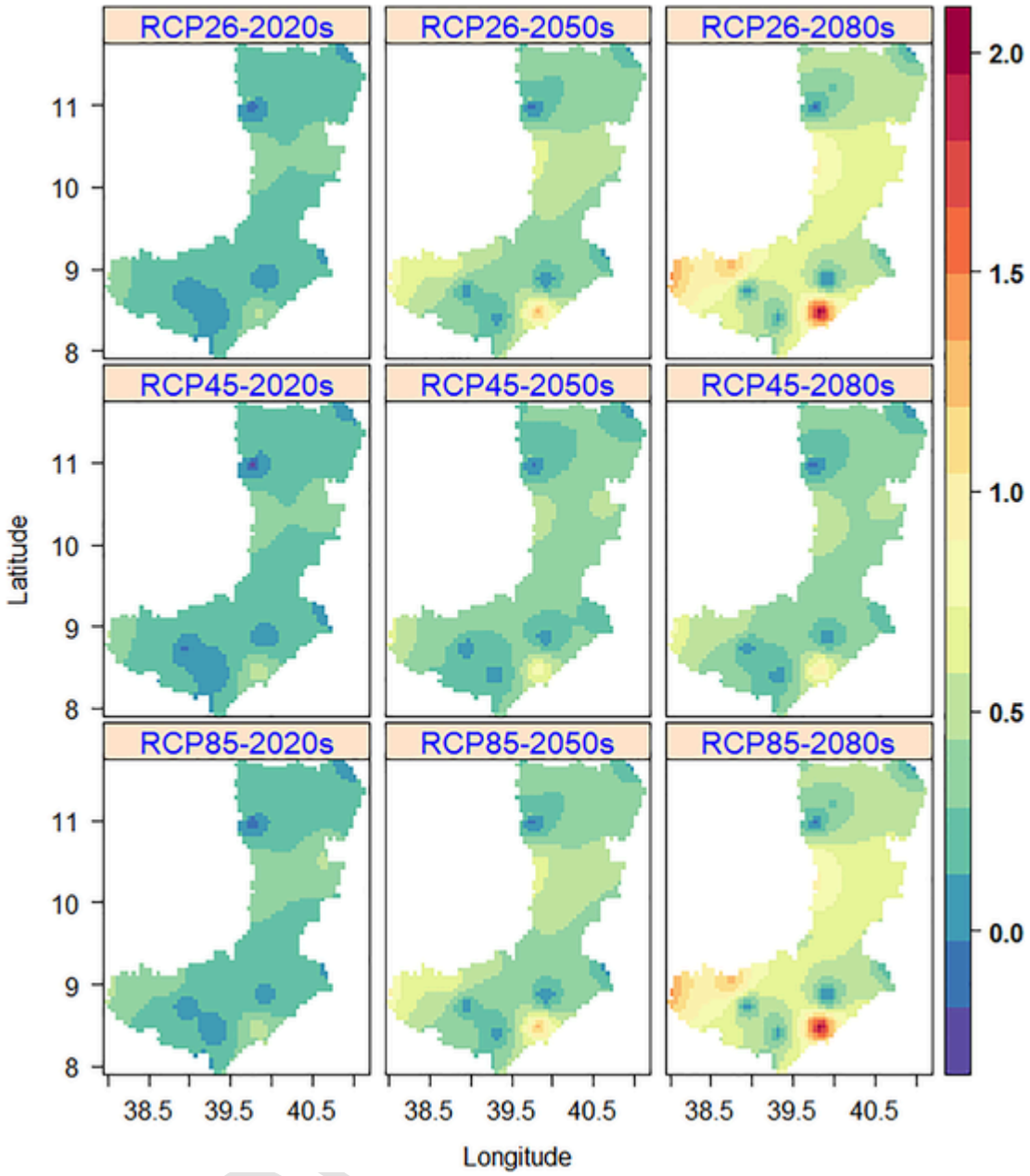

Fig. 4. Projected changes in Tmin (°C) in the 2020s (left), 2050s (middle) and 2080s (right) under RCP2.6 (upper), RCP4.5 (middle) and RCP8.5 (lower).

Similar to the projected change in Tmax, Tmin will be higher than the baseline period in large parts of the basin (Fig. 4). In the 2020s, large parts of the basin will be warmer (up to 0.65 °C) than the baseline period. Tmin will continue to increase in the 2050s (up to 1.6 °C) and 2080s (up to 2.05 °C). Compared to the 2020s and 2050s, the change in Tmin is higher in the 2080s, particularly under RCP2.6 and RCP8.5. Taking the basin average (Fig. 6), Tmin in the 2020s will be warmer than the baseline period by 0.19 °C, 0.18 °C, and 0.21 °C under RCP2.6, RCP4.5, and RCP8.5, respectively. Similarly, Tmin in the 2050s and 2080s will increase by more than 0.22 °C, 0.28 °C, and 0.36 °C under RCP2.6, RCP4.5, and RCP8.5, respectively.

The average annual precipitation show an increase, compared to the baseline period, in large parts of the basin in the 2020s, 2050s and 2080s under RCP2.6, RCP4.5, and RCP8.5 (Fig. 5). In the 2020s, the average annual precipitation will increase up to 310 mm and will continue to increase in the 2050s (up to 450 mm) and the 2080s (up 810 mm). The projected change in precipitation is higher in the 2080s compared to 2020s and 2050s, particularly under RCP8.5 around Koka dam and eastern part of Tendaho reservoir. Taking the basin average (Fig. 6), annual precipitation will be higher than it was during the baseline period by 10%, 11.7% and 13.4% under RCP2.6, RCP4.5 and RCP8.5, respectively. In addition, the average annual precipitation in the basin will increase by 16%, 18% and 25.8% under RCP2.6, RCP4.5 and RCP8.5, respectively in the 2050s. In the 2080s, the basin will be much wetter than the baseline period by 14%, 22% and 56% under RCP2.6, RCP4.5 and RCP8.5, respectively, which is higher than the 2020s and 2050s.

In line with the projected increase in precipitation, streamflow is projected to increase in the 2020s, 2050s, and 2080s under RCP2.6, RCP4.5, and RCP8.5 (Fig. 6). In the 2020s, streamflow is projected to increase by 40.7%, 34%, and 44.3% under RCP2.6, RCP4.5, and RCP8.5, respectively. Compared to the 2020s, the projected change in streamflow will be higher in the 2050s and 2080s. Compared to the ob-

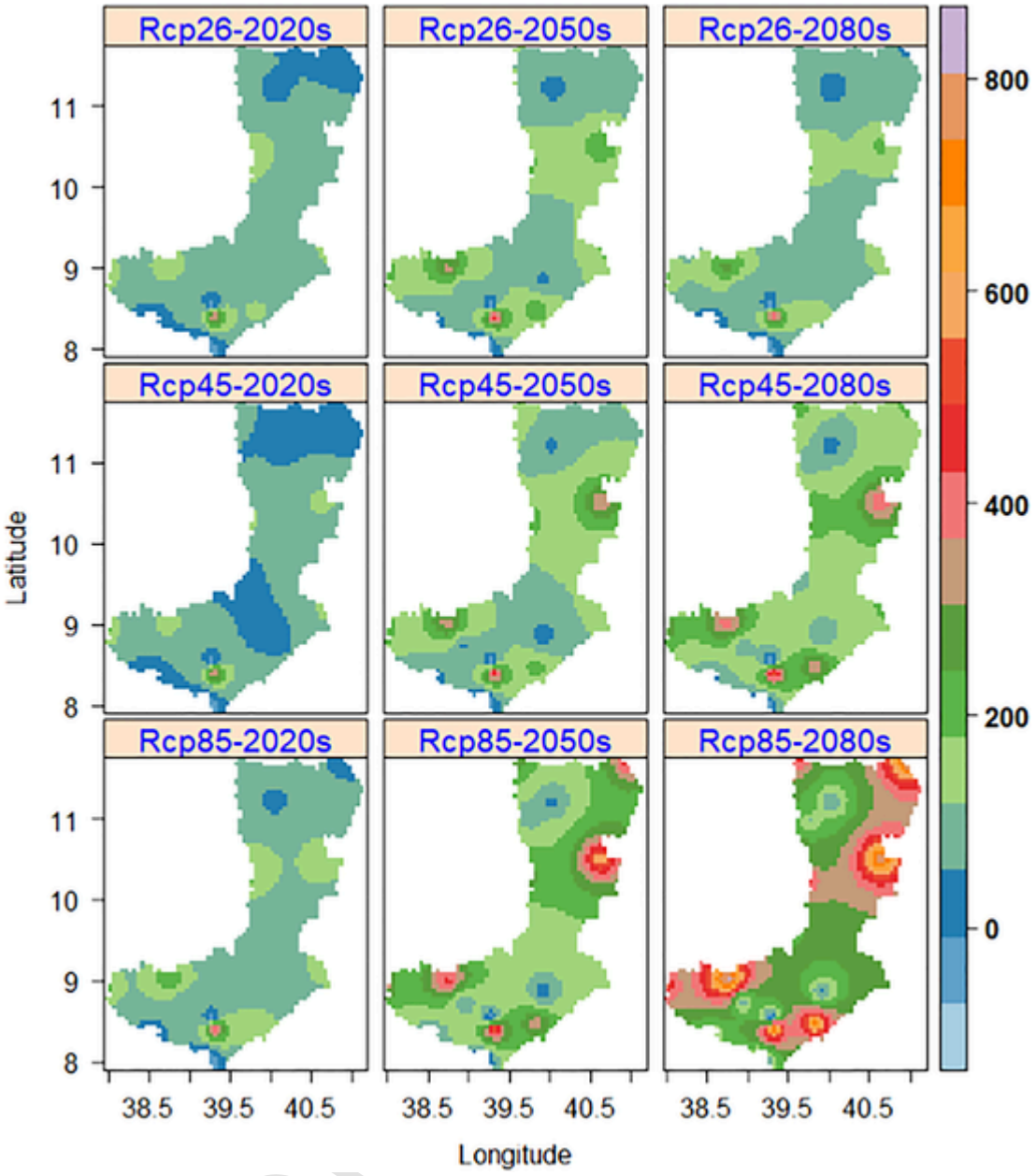

Fig. 5. Projected changes in precipitation (mm) in the 2020s (left), 2050s (middle) and 2080s (right) under RCP2.6 (upper), RCP4.5 (middle) and RCP8.5 (lower).

served flow (1990–2009), the projected flow will be higher by 50%, 57%, and 82% under RCP2.6, RCP4.5, and RCP8.5, respectively. Similarly, streamflow in the 2080s will be higher than the observed flow by 45%, 66%, and 191.6% under RCP2.6, RCP4.5, and RCP8.5, respectively.

On a seasonal time scale, streamflow is projected to increase during MAM and JJAS but decrease during JF and OND (Table 2). During MAM, streamflow will increase by more than 1.4%, 58%, and 42.4% in the 2020s, 2050s, and 2080s, respectively under the RCPs. Moreover, streamflow is projected to increase during JJAS by more than 23.7%, 51.6%, and 61.2% in the 2020s, 2050s, and 2080s, respectively. However, it is projected to decrease during OND and JF by more than 12.7% and 6.3% and 43.6% and 25.4% in the 2020s and 2050s, respectively. In the 2080s, streamflow will increase by 26.7% and 85% s during JF and OND, respectively under RCP8.5 but decrease under RCP2.6 and RCP4.5 by more than 24%.

4. Discussion

To tackle the possible impact of future climate change, particularly the change in precipitation, on sectors such as agriculture and water resources, observed and projected climate data with high spatial and temporal (e.g., daily) resolution are required to develop and drive impact assessment models. However, observed data from field-based meteorological stations, particularly in developing countries of East Africa are limited in terms of density, quality and accessibility, which hinders detailed impact assessment studies and development of site-specific adaptation measures. According to Wilby and Yu (2013), areas with limited ground information are the most vulnerable to climate change threats and it is recommended to use high-quality satellite and reanalysis based climate data products (Chaney et al., 2014; Gebrechorkos et al., 2019a; Jiang and Wang, 2019; Ma et al., 2018). Hydrological modelling using satellite-based climate data products can support mitigating the impacts of climate extremes and provide a better under-

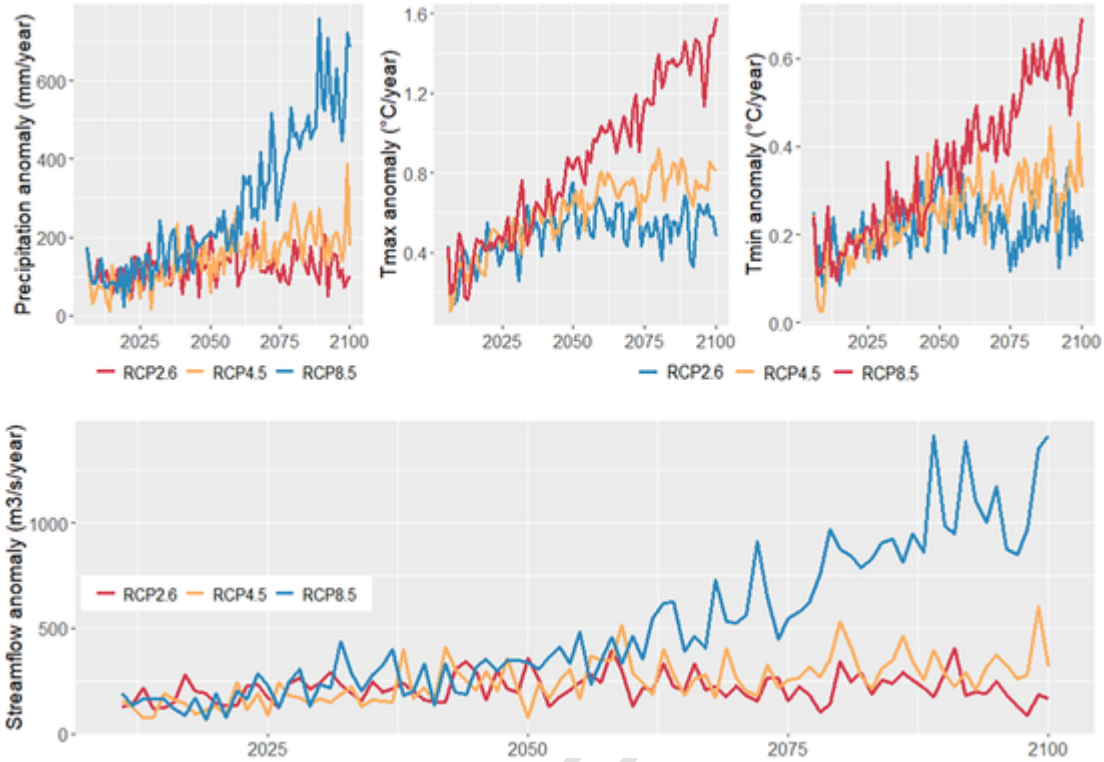

Fig. 6. Projected changes in basin average annual precipitation (mm, top left), Tmax (°C, top middle), Tmin (°C, top right) and streamflow (m^3/s, lower panel) for the period 2010–2100 under RCP2.6, RCP4.5, and RCP8.5.

Table 2
Projected changes in average seasonal flow (%) in the 2020s, 2050s, and 2080s under RCP2.6, RCP4.5, and RCP8.5.

Climate periods	RCP	JF	MAM	JJAS	OND
2020s	RCP2.6	−43.60	1.14	32.73	−13.12
	RCP4.5	−47.56	14.88	23.72	−18.11
	RCP8.5	−44.78	22.92	34.56	−12.73
2050s	RCP2.6	−45.35	58.10	51.58	−20.44
	RCP4.5	−52.24	79.60	59.20	−17.54
	RCP8.5	−25.40	141.26	78.51	−6.34
2080s	RCP2.6	−53.40	42.38	61.22	−31.09
	RCP4.5	−44.43	115.94	78.62	−23.84
	RCP8.5	26.68	401.67	162.80	84.71

standing in catchment water balance and management of water resources (Ma et al., 2018) and runoff predictions in large-scale catchments (Jiang and Wang, 2019).

In hydrological modelling, precipitation, compared to the other variables, is the most important component of the hydrological cycle and poor observations significantly affect the modelling process (Jiang and Wang, 2019). Moreover, poor rainfall products such as satellite-based rainfall estimations can lead to large uncertainties and biases in streamflow modelling. These limitations can be reduced by using high-quality products, blended with ground stations, and spatial downscaling for model calibration (Tan et al., 2014). Hence, all available climate data products can not directly be used in hydrological modelling and require a comprehensive evaluation with ground observation before being used in hydrological modelling to reduce biases and uncertainties. In Awash Basin, due to the limited availability of ground stations, studies were limited to sub-basins, particularly around the vicinity of meteorological stations (Gebrechorkos et al., 2019a; Mulugeta et al., 2019), but the application of high-quality climate datasets allow covering large basins. Considering the above recommendations, we used ground station data and the most accurate precipitation and temperature products recommended for East Africa (Basheer and Elagib, 2019; Gebrechorkos et al., 2018b) as it has been similarly practised with other data products in the basin (Mulugeta et al., 2019). In addition to the hydrological modelling, the selected rainfall and temperature products are used to statistically downscale climate projection from a GCM in data-sparse areas of the basin and this is considered as the best option to bridge the data gap (Wilby and Yu, 2013) and show a high correlation with observed data (Gebrechorkos et al., 2019c).

Using the statistically downscaled climate data, the results show an increase in annual average Tmax, Tmin, and precipitation in the 2020s, 2050s, and 2080s under RCP26-RCP8.5. The projected warming is in line with the most recent studies covering large parts of the basin (Engelbrecht et al., 2015; Osima et al., 2018; Pachauri et al., 2014) and with the observed warming of the region (Mulugeta et al., 2019). Moreover, precipitation is projected to increase by more than 10%, 16% and 14% in the 2020s, 2050s, and 2080s, respectively and this agrees with Tadese et al. (2019), which showed an increase, based on GCMs, in precipitation in 2050s and 2070s under RCP4.5 and high variability throughout the 21 century. Looking at the projected Tmax, Tmin, and precipitation, the change is higher in the 2050s and continues to increase, particularly under RCP8.5 and this is linked to the expected increase in the concentration of greenhouse gases after 2050s (IPCC, 2013).

Considering the hydrological modelling, our results confirm that the use of high-quality climate data products significantly improves the hydrological model accuracy (increase in correlation and reduce errors) by more than 25% (Table 2). For example, at station Melka-Kuntrea, the R^2 and NSE have increased from 0.67 and 0.67 to 0.86 and 0.84, respectively and the percentage of bias has decreased from 13.9% to 12.5%. Water management in this basin is very poor and the amount of water abstraction for irrigation and other purpose is not registered. Due

to the limited available information, such as water used for irrigation and for other sectors, required to accurately calibrate the model, most studies focus on the upper part of the basin (Chan et al., 2020; Gebrechorkos et al., 2019a; Mersha et al., 2018). Thus, the model accuracy decreases with an increase in drainage area (e.g., from Melka-Kuntrea to Tendaho) due to a large amount of water abstracted (e.g. for irrigation) and not included during the calibration and validation of the hydrological model. In data-limited basins, however, calibrated parameters from gauged areas of a similar region (e.g., with regard to hydrology and topography) can be transferred, which is also called regionalization of model parameters, to ungauged areas (Bárdossy, 2007; Blöschl, 2006). Therefore, even though the model shows a satisfactory performance at the downstream part of the basin, the calibrated model with a very good performance at the upper-part should represent the downstream part of the basin as well. Overall, according to other studies in this field (Almeida et al., 2018; Fernandez et al., 2005; Gessesse et al., 2019; Motovilov et al., 1999; Yanto et al., 2017), the calibrated and validated model is classified as satisfactory (e.g., station Melka-Selki) to very-good (e.g., station Melka-Kuntrea). Alazzy et al. (2017) concluded that application of high-quality rainfall products in hydrological models produces comparable results to data from ground stations.

In line with the projected change in precipitation, the average annual streamflow is projected to increase by more than 34%, 50.4%, and 45.1% in the 2020s, 2050s and 2080s, respectively. The projected increase in average annual streamflow is in line with previous studies in sub-basins of the Awash River basin, which showed an increase up to 150% (Gebrechorkos et al., 2019a; Tadese et al., 2019). On a seasonal time scale, streamflow will increase by more than 2 m^3/s and 200 m^3/s during March–May (MAM) and June–September (JJAS), respectively but decrease during January–February (JF) and October–December (OND) seasons. In line to this study, hydrological projection in the Awash basin shows an increase in streamflow by more than 10–51% during JJAS by 2080s (Hirpa et al., 2019). Even though projections are showing an increase in streamflow, temperature and evapotranspiration are projected to increase in basins of East Africa (Berhe et al., 2013; Gebrechorkos et al., 2019a). In the Awash basin, the amount of water loss by evapotranspiration is greater than 72% of the total water is used for irrigation (Berhe et al., 2013).

Water stress, particularly during dry seasons, lead to an increase in food insecurity as a result of a significant reduction in crop productivity and death of livestock (Murendo et al., 2011; Taye et al., 2018). In general, a decrease in rainfall (e.g. 5%) strongly affects the Growth Domestic Product (GDP) and agricultural productivity of the basin by 5% and 10%, respectively (Borgomeo et al., 2018). Based on GCMs projection, it is also concluded that water availability (precipitation - potential evapotranspiration) in this basin is projected to decrease under the high emission scenario (RCP 8.5) during the 2020s–2080s (Taye et al., 2018). Hence, considering the projected warming in temperature (increase in Tmax and Tmin), variability in rainfall, and decrease in streamflow during JF and OND seasons it is required to develop management and adaptation measures (e.g., construction of dams), water allocation system, and watershed management practices to reduce the negative impact of climate change on the agriculture and other sectors.

5. Conclusions

The plausible hydrological impact of climate change was assessed in one of the largest, agricultural intensive and economically important, but data-scarce areas of Ethiopia during the period from the 2020s to 2080s under three different climate change scenarios (RCPs). We used observed and satellite and reanalysis based climate datasets, identified after a comprehensive evaluation, available at higher spatial and temporal resolution and for longer periods. A location-based climate projection, equivalent to future station data, was developed by statistical downscaling using SDSM from a GCM and fed to a hydrological model, for the first time in the basin, to assess the possible impact of climate change, particularly changes Tmax, Tmin, and precipitation on the hydrology of the basin. Both the climate (SDSM) and hydrological (SWAT) models were calibrated and validated using observed climate and hydrological data. The application of additional climate datasets, in addition to an increase in the study area where station data is unavailable, improved the accuracy of the hydrological modelling by more than 25%.

The results show an increase in average annual Tmax, Tmin, and precipitation in the 2020s, 2050s, and 2080s. The projected change is higher under RCP8.5 and after 2050 due to the expected increase in greenhouse gases concentration. In line with the projected increase in precipitation, annual streamflow will increase by an average of more than 10% in the 2020s, 2050s and 2080s under the RCPs (RCP2.6, RCP4.5, and RCP8.5). On the seasonal scale, streamflow is projected to decrease during the dry (JF) and short-rainy (OND) seasons in the 2020s–2080s. However, it is projected to increase during the long-rainy (MAM) and June–September (JJAS) seasons throughout the 21 century under the three RCPs. In general, streamflow will increase during wet and decrease during dry months and seasons. Overall, the projected decrease in streamflow during the dry seasons and increase in temperature signals the increase in water stress, which might affect the regions food and water security and reduce irrigation related investment in the basin. Therefore, it is important to advance the knowledge and capacity of the local farmers by providing training on water management and water allocation systems and farming systems (e.g., cropping pattern), and strengthen the farmers and regional meteorological office relationship in a way to get up-to-date seasonal forecasting information to prepare to the changes in advance. Overall, considering projected hydro-climate changes and increase in population and related demand for water, food, and energy, it is crucial to act now to develop climate change adaptation measures in the region to minimize the impacts.

Supplementary data to this article can be found online at https://doi.org/10.1016/j.scitotenv.2020.140504.

CRediT authorship contribution statement

Solomon H. Gebrechorkos: Methodology, Investigation, Formal analysis, Writing - original draft.**Christian Bernhofer:**Methodology, Writing - original draft.**Stephan Hülsmann:**Methodology, Writing - original draft.

Declaration of competing interest

The authors declare that they have no known competing financial interests or personal relationships that could have appeared to influence the work reported in this paper.

References

Abbaspour, K C, 2015. SWAT Calibration and Uncertainty Programs 100.
Adhikari, U, Nejadhashemi, A P, Woznicki, S A, 2015. Climate change and eastern Africa: a review of impact on major crops. Food Energy Secur 4, 110–132. doi:10.1002/fes3.61.
Alazzy, A A, Lü, H, Chen, R, Ali, A B, Zhu, Y, Su, J, 2017. Evaluation of satellite precipitation products and their potential influence on hydrological modeling over the Ganzi River basin of the Tibetan Plateau [WWW document]. Adv. Meteorol.. doi:10.1155/2017/3695285.
Almeida, R A, Pereira, S B, Pinto, D B F, Almeida, R A, Pereira, S B, Pinto, D B F, 2018. Calibration and validation of the swat hydrological model for the Mucuri River basin. Eng. Agríc. 38, 55–63. doi:10.1590/1809-4430-eng.agric.v38n1p55-63/2018.
Ayenew, T, Kebede, S, Alemyahu, T, 2008. Environmental isotopes and hydrochemical study applied to surface water and groundwater interaction in the Awash River basin. Hydrol. Process. 22, 1548–1563. doi:10.1002/hyp.6716.
Ayugi, B, Tan, G, Ullah, W, Boiyo, R, Ongoma, V, 2019. Inter-comparison of remotely sensed precipitation datasets over Kenya during 1998–2016. Atmospheric Res 225, 96–109. doi:10.1016/j.atmosres.2019.03.032.
Bárdossy, A, 2007. Calibration of hydrological model parameters for ungauged catchments. Hydrol. Earth Syst. Sci. 11, 703–710. doi:10.5194/hess-11-703-2007.

Basheer, M, Elagib, N A, 2019. Performance of satellite-based and GPCC 7.0 rainfall products in an extremely data-scarce country in the Nile Basin. Atmospheric Res 215, 128–140. doi:10.1016/j.atmosres.2018.08.028.

Behera, S, Khare, D, Mishra, P, Sahoo, S, 2016. Application of Statistical Downscaling Model for Prediction of Future Rainfall in Bhudhabalanga River Basin, Odisha (India) [WWW Document]. URL/paper/Application-of-Statistical-Downscaling-Model-for-of-Behera-Khare/edf555da939a5bad648c7b07bd7e3d089a5727d3 (accessed 6.8.20).

Berhe, F T, Melesse, A M, Hailu, D, Sileshi, Y, 2013. MODSIM-based water allocation modeling of Awash River basin, Ethiopia. Catena 109, 118–128. doi:10.1016/j.catena.2013.04.007.

Blöschl, G, 2006. Rainfall-runoff modeling of ungauged catchments. In: Encyclopedia of Hydrological Sciences. American Cancer Society. doi:10.1002/0470848944.hsa140.

Borgomeo, E, Vadheim, B, Woldeyes, F B, Alamirew, T, Tamru, S, Charles, K J, Kebede, S, Walker, O, 2018. The distributional and multi-sectoral impacts of rainfall shocks: evidence from computable general equilibrium modelling for the Awash Basin, Ethiopia. Ecol. Econ. 146, 621–632. doi:10.1016/j.ecolecon.2017.11.038.

Bosch, N S, Allan, J D, Dolan, D M, Han, H, Richards, R P, 2011. Application of the soil and water assessment tool for six watersheds of Lake Erie: model parameterization and calibration. J. Gt. Lakes Res. 37, 263–271. doi:10.1016/j.jglr.2011.03.004.

Brown, M E, Funk, C C, 2008. Food security under climate change. Science 319, 580–581. doi:10.1126/science.1154102.

Camberlin, P, 2017. Temperature trends and variability in the greater horn of Africa: interactions with precipitation. Clim. Dyn. 48, 477–498. doi:10.1007/s00382-016-3088-5.

Cattani, E, Merino, A, Guijarro, J A, Levizzani, V, 2018. East Africa rainfall trends and variability 1983–2015 using three long-term satellite products. Remote Sens. 10, 931. doi:10.3390/rs10060931.

Chan, W C H, Thompson, J R, Taylor, R G, Nay, A E, Ayenew, T, MacDonald, A M, Todd, M C, 2020. Uncertainty assessment in river flow projections for Ethiopia's upper Awash Basin using multiple GCMs and hydrological models. Hydrol. Sci. J. (0) null. doi:10.1080/02626667.2020.1767782.

Chaney, N W, Sheffield, J, Villarini, G, Wood, E F, 2014. Development of a high-resolution gridded daily meteorological dataset over sub-Saharan Africa: spatial analysis of trends in climate extremes. J. Clim. 27, 5815–5835. doi:10.1175/JCLI-D-13-00423.1.

Coulibaly, P, Dibike, Y B, Anctil, F, 2005. Downscaling precipitation and temperature with temporal neural networks. J. Hydrometeorol. 6, 483–496. doi:10.1175/JHM409.1.

Dile, T Y, Srinivasan, R, 2014. Evaluation of CFSR climate data for hydrologic prediction in data-scarce watersheds: an application in the Blue Nile River basin. JAWRA J. Am. Water Resour. Assoc. 50, 1226–1241. doi:10.1111/jawr.12182.

Engelbrecht, F, Adegoke, J, Bopape, M-J, Naidoo, M, Garland, R, Thatcher, Marcus, McGregor, J, Katzfey, J, Werner, M, Ichoku, C, Gatebe, C, 2015. Projections of rapidly rising surface temperatures over Africa under low mitigation. Environ. Res. Lett. 10, 85004. doi:10.1088/1748-9326/10/8/085004.

FAO, 2014. The State of Food Insecurity in the World (SOFI). Food and Agricultural Organization of the United Nations and World Bank.

Fenta, A A, Yasuda, H, Shimizu, K, Haregeweyn, N, Kawai, T, Sultan, D, Ebabu, K, Belay, A S, 2017. Spatial distribution and temporal trends of rainfall and erosivity in the Eastern Africa region. Hydrol. Process. 31, 4555–4567. doi:10.1002/hyp.11378.

Fernandez, G P, Chescheir, G M, Skaggs, R W, Amatya, D M, 2005. Development and Testing of Watershed-scale Models for Poorly Drained Soils.

Fischer, G, Nachtergaele, F O, Prieler, S, van Velthuizen, H, Verelst, L, Wiberg, D, 2008. Global Agro-ecological Zones Global Agro-ecological Zones Assessment for Agriculture (Other). IIASA, Laxenburg, Austria and FAO, Rome Italy.

Fowler, H J, Wilby, R L, 2007. Beyond the downscaling comparison study. Int. J. Climatol. 27, 1543–1545. doi:10.1002/joc.1616.

Fuka, D R, Walter, M T, MacAlister, C, Degaetano, A T, Steenhuis, T S, Easton, Z M, 2014. Using the climate forecast system reanalysis as weather input data for watershed models. Hydrol. Process. 28, 5613–5623. doi:10.1002/hyp.10073.

Funk, C, Peterson, P, Landsfeld, M, Pedreros, D, Verdin, J, Shukla, S, Husak, G, Rowland, J, Harrison, L, Hoell, A, Michaelsen, J, 2015. The climate hazards infrared precipitation with stations—a new environmental record for monitoring extremes. Sci. Data 2, 150066. doi:10.1038/sdata.2015.66.

Gebrechorkos, S H, Hülsmann, S, Bernhofer, C, 2018. Changes in temperature and precipitation extremes in Ethiopia, Kenya, and Tanzania. Int. J. Climatol. 39, 18–30. doi:10.1002/joc.5777.

Gebrechorkos, S H, Hülsmann, S, Bernhofer, C, 2018. Evaluation of multiple climate data sources for managing environmental resources in East Africa. Hydrol. Earth Syst. Sci. 22, 4547–4564. doi:10.5194/hess-22-4547-2018.

Gebrechorkos, S H, Bernhofer, C, Hülsmann, S, 2019. Impacts of projected change in climate on water balance in basins of East Africa. Sci. Total Environ.. doi:10.1016/j.scitotenv.2019.05.053.

Gebrechorkos, S H, Hülsmann, S, Bernhofer, C, 2019. Regional climate projections for impact assessment studies in East Africa. Environ. Res. Lett. 14, 044031. doi:10.1088/1748-9326/ab055a.

Gebrechorkos, S H, Hülsmann, S, Bernhofer, C, 2019. Statistically downscaled climate dataset for East Africa. Sci. Data 6, 31. doi:10.1038/s41597-019-0038-1.

Gessesse, A A, Melesse, A M, Abera, F F, Abiy, A Z, 2019. Modeling hydrological responses to land use dynamics, choke, Ethiopia. Water Conserv. Sci. Eng. 4, 201–212. doi:10.1007/s41101-019-00076-3.

Girvetz, E, Ramirez-Villegas, J, Claessens, L, Lamanna, C, Navarro-Racines, C, Nowak, A, Thornton, P, Rosenstock, T S, 2019. Future climate projections in Africa: where are we headed? In: Rosenstock, T S, Nowak, A, Girvetz, E (Eds.), The Climate-Smart Agriculture Papers: Investigating the Business of a Productive, Resilient and Low Emission Future. Springer International Publishing, Cham, pp. 15–27. doi:10.1007/978-3-319-92798-5_2.

Goodess, C M, Anagnostopoulou, C, Bárdossy, A, Frei, C, Harpham, C, Haylock, M R, Hundecha, Y, Maheras, P, Ribalaygua, J, Schmidli, J, Schmith, T, Tolika, K, Tomozeiu, R, 2012. An Intercomparison of Statistical Downscaling Methods for Europe and European Regions – Assessing Their Performance With Respect to Extreme Temperature and Precipitation Events.

Guo, Y, Fang, G, Xu, Y-P, Tian, X, Xie, J, 2020. Identifying how future climate and land use/cover changes impact streamflow in Xinanjiang Basin, East China. Sci. Total Environ. 710, 136275. doi:10.1016/j.scitotenv.2019.136275.

Gutmann, E D, Rasmussen, R M, Liu, C, Ikeda, K, Gochis, D J, Clark, M P, Dudhia, J, Thompson, G, 2012. A comparison of statistical and dynamical downscaling of winter precipitation over complex terrain. J. Clim. 25, 262–281. doi:10.1175/2011JCLI4109.1.

Haile, G G, Tang, Q, Leng, G, Jia, G, Wang, J, Cai, D, Sun, S, Baniya, B, Zhang, Q, 2020. Long-term spatiotemporal variation of drought patterns over the Greater Horn of Africa. Sci. Total Environ. 704, 135299. doi:10.1016/j.scitotenv.2019.135299.

Hashmi, M Z, Shamseldin, A Y, Melville, B W, 2011. Comparison of SDSM and LARS-WG for simulation and downscaling of extreme precipitation events in a watershed. Stoch. Environ. Res. Risk Assess. 25, 475–484. doi:10.1007/s00477-010-0416-x.

Hassan, Z, Shamsudin, S, Harun, S, 2013. Application of SDSM and LARS-WG for simulating and downscaling of rainfall and temperature. Theor. Appl. Climatol. 116, 243–257. doi:10.1007/s00704-013-0951-8.

Hirpa, F A, Gebremichael, M, Hopson, T, 2009. Evaluation of high-resolution satellite precipitation products over very complex terrain in Ethiopia. J. Appl. Meteorol. Climatol. 49, 1044–1051. doi:10.1175/2009JAMC2298.1.

Hirpa, F A, Alfieri, L, Lees, T, Peng, J, Dyer, E, Dadson, S J, 2019. Streamflow response to climate change in the Greater Horn of Africa. Clim. Chang. 156, 341–363. doi:10.1007/s10584-019-02547-x.

IPCC, 2007. In: Solomon, S (Ed.), et al., Climate Change 2007: The Physical Science Basis. Cambridge Univ. Press (WG1).

IPCC, 2013. In: Stocker (Ed.), et al., Climate Change 2013: The Physical Science Basis. Cambridge Univ Press (WG1).

Jiang, D, Wang, K, 2019. The role of satellite-based remote sensing in improving simulated streamflow: a review. Water 11, 1615. doi:10.3390/w11081615.

Joetzjer, E, Douville, H, Delire, C, Ciais, P, 2013. Present-day and future Amazonian precipitation in global climate models: CMIP5 versus CMIP3. Clim. Dyn. 41, 2921–2936. doi:10.1007/s00382-012-1644-1.

Khan, M S, Coulibaly, P, 2009. Assessing hydrologic impact of climate change with uncertainty estimates: Bayesian neural network approach. J. Hydrometeorol. 11, 482–495. doi:10.1175/2009JHM1160.1.

Liu, Z, Xu, Z, Charles, S P, Fu, G, Liu, L, 2011. Evaluation of two statistical downscaling models for daily precipitation over an arid basin in China. Int. J. Climatol. 31, 2006–2020. doi:10.1002/joc.2211.

Liu, J, Yuan, D, Zhang, L, Zou, X, Song, X, 2015. Comparison of three statistical downscaling methods and ensemble downscaling method based on Bayesian model averaging in upper Hanjiang River basin, China [WWW document]. Adv. Meteorol.. doi:10.1155/2016/7463963.

Luo, Y, Ficklin, D L, Liu, X, Zhang, M, 2013. Assessment of climate change impacts on hydrology and water quality with a watershed modeling approach. Sci. Total Environ. 450–451, 72–82. doi:10.1016/j.scitotenv.2013.02.004.

Lutz, A F, ter Maat, H W, Biemans, H, Shrestha, A B, Wester, P, Immerzeel, W W, 2016. Selecting representative climate models for climate change impact studies: an advanced envelope-based selection approach. Int. J. Climatol. 36, 3988–4005. doi:10.1002/joc.4608.

Ma, J, Sun, W, Yang, G, Zhang, D, 2018. Hydrological analysis using satellite remote sensing big data and CREST model. IEEE Access 6, 9006–9016. doi:10.1109/ACCESS.2018.2810252.

Mejia, J F, Huntington, J, Hatchett, B, Koracin, D, Niswonger, R G, 2012. Linking global climate models to an integrated hydrologic model: using an individual station downscaling approach. J. Contemp. Water Res. Educ., Universities Council on Water Resources 17–27.

Mersha, A N, Masih, I, De Fraiture, C, Wenninger, J, Alamirew, T, 2018. Evaluating the impacts of IWRM policy actions on demand satisfaction and downstream water availability in the Upper Awash Basin, Ethiopia. Water 10, 892. doi:10.3390/w10070892.

Motovilov, Y G, Gottschalk, L, Engeland, K, Rodhe, A, 1999. Validation of a distributed hydrological model against spatial observations. Agric. For. Meteorol. 98–99, 257–277. doi:10.1016/S0168-1923(99)00102-1.

Mulugeta, S, Fedler, C, Ayana, M, 2019. Analysis of long-term trends of annual and seasonal rainfall in the Awash River basin, Ethiopia. Water 11, 1498. doi:10.3390/w11071498.

Murendo, C, Keil, A, Zeller, M, 2011. Drought impacts and related risk management by smallholder farmers in developing countries: evidence from Awash River basin, Ethiopia. Risk Manage 13, 247–263. doi:10.1057/rm.2011.17.

Nash, J E, Sutcliffe, J V, 1970. River flow forecasting through conceptual models part I — a discussion of principles. J. Hydrol. 10, 282–290. doi:10.1016/0022-1694(70)90255-6.

Neitsch, S L, Arnold, J G, Kiniry, J R, Williams, J R, 2011. Soil and Water Assessment Tool Theoretical Documentation Version 2009 (Technical Report). Texas Water Resources Institute.

Niang, I, Ruppel, O C, Abdrabo, M A, Essel, A, Lennard, C, Padgham, J, Urquhart, P, 2014. Africa. In: Barros, V R (Ed.), et al., Climate Change 2014: Impacts, Adaptation, and Vulnerability. Part B: Regional Aspects. Cambridge Univ. Press (WG2).

Osima, S, Indasi, V S, Zaroug, M, Endris, H S, Gudoshava, M, Misiani, H O, Nimusiima, A, Anyah, R O, Otieno, G, Ogwang, B A, Jain, S, Kondowe, A L, Mwangi, Emmah, Lennard, C, Nikulin, G, Dosio, A, 2018. Projected climate over the Greater Horn of Africa under 1.5 °C and 2 °C global warming. Environ. Res. Lett. 13, 065004. doi:10.1088/1748-9326/aaba1b.

Pachauri, R K, Allen, M R, Barros, V R, Broome, J, Cramer, W, Christ, R, Church, J A, Clarke, L, Dahe, Q, Dasgupta, P, Dubash, N K, Edenhofer, O, Elgizouli, I, Field, C B, Forster, P, Friedlingstein, P, Fuglestvedt, J, Gomez-Echeverri, L, Hallegatte, S, Hegerl, G, Howden, M, Jiang, K, Jimenez Cisneroz, B, Kattsov, V, Lee, H, Mach, K J, Marotzke, J, Mastrandrea, M D, Meyer, L, Minx, J, Mulugetta, Y, O'Brien, K, Oppenheimer, M, Pereira, J J, Pichs-Madruga, R, Plattner, G-K, Pörtner, H-O, Power, S B, Preston, B, Ravindranath, N H, Reisinger, A, Riahi, K, Rusticucci, M, Scholes, R, Seyboth, K, Sokona, Y, Stavins, R, Stocker, T F, Tschakert, P, van Vuuren, D, van Ypserle, J-P, 2014. Climate Change 2014: Synthesis Report. Contribution of Working Groups I, II and III to the Fifth Assessment Report of the Intergovernmental Panel on Climate Change, EPIC3Geneva, Switzerland, IPCC 151 p. IPCC, Geneva, Switzerland, p. 151 ISBN: 978-92-9169-143-2.

Schnorbus, M A, Cannon, A J, 2014. Statistical emulation of streamflow projections from a distributed hydrological model: application to CMIP3 and CMIP5 climate projections for British Columbia, Canada. Water Resour. Res. 50, 8907–8926. doi:10.1002/2014WR015279.

Sheffield, J, Goteti, G, Wood, E F, 2006. Development of a 50-year high-resolution global dataset of meteorological forcings for land surface modeling. J. Clim. 19, 3088–3111. doi:10.1175/JCLI3790.1.

Tadese, M T, Kumar, L, Koech, R, 2019. Climate change projections in the Awash River basin of Ethiopia using global and regional climate models. Int. J. Climatol. n/a.. doi:10.1002/joc.6418.

Tan, M L, Latif, A B, Pohl, C, Duan, Z, 2014. Streamflow modelling by remote sensing: a contribution to digital Earth. IOP Conf. Ser. Earth Environ. Sci. 18, 012060. doi:10.1088/1755-1315/18/1/012060.

Tavakol-Davani, H, Nasseri, M, Zahraie, B, 2012. Improved statistical downscaling of daily precipitation using SDSM platform and data-mining methods. Int. J. Climatol. 33, 2561–2578. doi:10.1002/joc.3611.

Taye, M T, Dyer, E, Hirpa, F A, Charles, K, 2018. Climate change impact on water resources in the Awash Basin, Ethiopia. Water 10, 1560. doi:10.3390/w10111560.

Tryhorn, L, DeGaetano, A, 2011. A comparison of techniques for downscaling extreme precipitation over the Northeastern United States. Int. J. Climatol. 31, 1975–1989. doi:10.1002/joc.2208.

Wang, Y, Yang, X, Zhang, M, Zhang, L, Yu, X, Ren, L, Liu, Y, Jiang, S, Yuan, F, 2019. Projected effects of climate change on future hydrological regimes in the upper Yangtze River basin, China [WWW document]. Adv. Meteorol.. doi:10.1155/2019/1545746.

Wilby, R L, Dawson, C W, 2004. sdsm — a decision support tool for the assessment of regional climate change impacts. Environ. Model. Softw. 17, 145–157. doi:10.1016/S1364-8152(01)00060-3.

Wilby, R L, Dawson, C W, 2013. The statistical downscaling model: insights from one decade of application. Int. J. Climatol. 33, 1707–1719. doi:10.1002/joc.3544.

Wilby, R L, Yu, D, 2013. Rainfall and temperature estimation for a data sparse region. Hydrol. Earth Syst. Sci. 17, 3937–3955. doi:10.5194/hess-17-3937-2013.

Wu, P, Christidis, N, Stott, P, 2013. Anthropogenic impact on Earth's hydrological cycle. Nat. Clim. Chang. 3, 807–810. doi:10.1038/nclimate1932.

Yanto Livneh, B, Rajagopalan, B, Kasprzyk, J, 2017. Hydrological model application under data scarcity for multiple watersheds, Java Island, Indonesia. J. Hydrol. Reg. Stud. 9, 127–139. doi:10.1016/j.ejrh.2016.09.007.